ISSN 1392–1320 MATERIALS SCIENCE (MEDŽIAGOTYRA). Vol. 28, No. 2. 2022

High Temperature Oxidation Behavior of New Martensitic Heat-Resistant Steel

Ziming BAO [1], Renheng HAN [1], Yanqing ZHU [1], Hong LI [1], Ning LI [1], Ming TANG [1], Hexin ZHANG [1, 2] *, Chengzhi ZHAO [1, 2]

[1] *College of Materials Science and Chemical Engineering, Harbin Engineering University, No. 145 Nantong Avenue, Harbin, Heilongjiang, 150001, China*
[2] *Key Laboratory of Superlight Materials and Surface Technology of Ministry of Education, Harbin Engineering University, No. 145 Nantong Avenue, Harbin, Heilongjiang, 150001, China*

crossref http://dx.doi.org/10.5755/j02.ms.27438

Received 03 August 2020; accepted 07 September 2020

The research focuses on the high temperature oxidation resistance of martensitic heat-resistant steel. A new type of martensitic heat-resistant steel was developed with the addition of Al and Cu, and the oxidation behavior of the new martensitic heat-resistant steel at 650 °C and 700 °C was analyzed. The high temperature oxidation kinetics curves of new martensitic heat-resistant steel at 650 °C and 700 °C were determined and plotted by cyclic oxidation experiment and discontinuous weighing method. XRD technique was applied to qualitatively analyze the surface oxide of the material after oxidation. The surface and cross-section morphology of the material were observed by field emission scanning electron microscope (SEM) and energy dispersive spectrometer (EDS), and the oxidation mechanism at high temperature was analyzed. The results show that the oxide film can be divided into two layers after oxidation at 650 ºC for 200 h. The outer oxide film is mainly composed of Fe and Cu oxides, and the inner oxide film is mainly composed of Al_2O_3, SiO_2 and Cr_2O_3. After oxidation at 700 ºC for 200 h, the outer layer is mainly composed of Fe, Cu, Mn oxides, and the inner layer is mainly composed of Cr, Al and Si oxides. The addition of a small amount of Cu promotes the diffusion of Al and Si elements, facilitates the formation of Al_2O_3 and SiO_2, and improves the high-temperature oxidation resistance of martensitic heat-resistant steel.

Keywords: heat-resistant steel, high temperature oxidation, morphology of oxide film, element distribution

1. INTRODUCTION

For the purpose of saving energy and reducing the consumption of thermal power units, unit parameters need to be continuously improved [1 – 4]. Superheater and resuperheater need to operate under higher temperature and higher pressure, and the subsequent oxidation problem is more prominent [5 – 9]. Thus, it is more important to study the composition, structure, morphology and formation rule of the oxide layer so as to effectively control the rapid growth and peeling of the oxide layer. Martensitic heat-resistant steel is often used for manufacturing high-temperature parts because of its good mechanical properties and relatively low cost. Due to the high ambient temperature and high stress of high temperature parts, Matrensitic heat-resistant steel can easily lose effectiveness during the pricess. Therefore, improving the performance of martensitic heat-resistant steel remains the key to improvement on work efficiency and service life [10].

At present, optimizing the heat treatment process and innovating chemical composition are the common ways to improve the service life of heat-resistant steel [11]. Martensitic heat-resistant steel uses Cr as the main element to improve corrosion resistance and oxidation resistance, and forms a variety of strengthening methods by adding other elements to improve high-temperature strength and structural stability [12]. It is found that at least 12 % Cr element [13, 14] should be added in order to form a strong and effective Cr_2O_3 protective layer for martensitic heat-resistant steel. When the content of Cr element is more than 12 %, the electrode potential of the steel will change from negative to positive, which will make it harder for iron atom to lose electrons, and a layer of smooth Cr-rich oxide will be formed on the surface of the steel, which improves the corrosion resistance of the steel [15]. However, the Cr content of the new martensitic heat-resistant steel used in this paper is less than 12 %, the addition of Al element can improve the high-temperature oxidation resistance of the heat-resistant steel [16]. The formation of Al_2O_3 oxide film under high-temperature conditions has a stronger protective effect than Cr_2O_3 [17]. In martensitic heat-resistant steel, with the increase of Cr in the matrix, the diffusion of Al on the surface of the oxide film increases [14]. The addition of Al element will lead to poor fluidity of alloy liquid and increase of hardness and brittleness of steel [18]. In this experiment, Cu element was added to further optimize the properties of martensitic heat-resistant steel. The addition of Cu element can improve the diffusion rate of Al element [19, 20], It has been proved that the addition of 3% Cu in Super304H [21] steel can produce copper rich phase precipitated in austenite during service, the fine Cu precipitate in the matrix can improve its high temperature strength, high temperature plasticity and high temperature oxidation resistance by refining grains [21 – 24]. In this paper, a new type of martensitic heat-resistant steel was prepared by adding a small amount of Al and Cu elements

* Corresponding author. Tel.: +86-13895718408.
E-mail address: *zhanghx@hrbeu.edu.cn* (H. Zhang)

into Fe-Cr martensitic heat-resistant steel. The oxidation kinetics curves and XRD patterns at 650 ºC and 700 ºC were measured. By observing and analyzing the oxidation morphology and oxidation cross-section, the high temperature oxidation resistance of the new martensitic heat-resistant steel was evaluated, which provided experimental basis for further composition optimization of martensitic heat-resistant steel.

2. MATERIALS AND METHODS

2.1. Materials

The new martensitic heat-resistant steel was melted in VIM500 vacuum non-consumable tungsten electrode melting furnace made by Shenyang Scientific Instrument Co, Ltd, Chinese Academy of Sciences. After melting, the material was processed into small pieces with a = 15 mm. The chemical composition of as cast new martensitic heat-resistant steel was determined by Spectro Maxx direct reading spectrometer. The results are shown in Table 1.

The new martensitic heat-resistant steel as cast was put into RJX-8-13 high-temperature box type resistance furnace for heat treatment. The heat treatment process is under 1050 °C for 0.75 h air cooling + 770 °C × 2 h with furnace cooling to 300 °C and then air cooling to room temperature. The heat treatment process diagram is shown in Fig. 1.

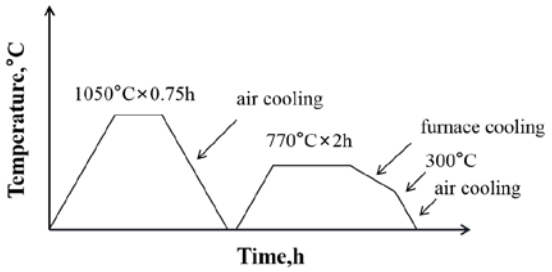

Fig. 1. Heat treatment process of new martensitic heat resistant steel

After heat treatment, the new martensitic heat-resistant steel was processed into small pieces of 20 mm × 10 mm × 2 mm by DK7745 wire cutting machine. The abrasive paper was used for rough grinding and fine grinding, and the polishing machine was used to polish the sample. The corrosion solution was 4 g picric acid + 5 ml hydrochloric acid + 100 ml alcohol mixture solution. The microstructure of the new martensitic heat-resistant steel after corrosion is shown in Fig. 2.

2.2. Methods

In the high temperature oxidation experiment, the Mao Fu type resistance furnace SM-28-10 was used for heating, and the alumina crucible was used to load the samples. The experimental temperature was 650 °C and 700 °C, and the oxidation time was 200 h. Samples were taken out for weighing measurement at regular intervals. An electronic analytical balance with an accuracy of 1×10^{-4} g was used to weigh the sample mass.

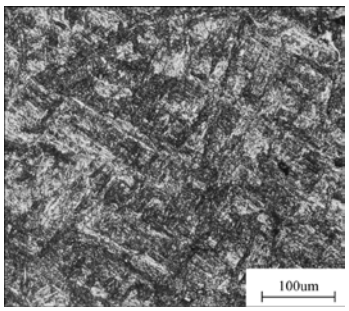

Fig. 2. Microstructure of new martensitic heat resistant steel

The oxidation kinetics curve was drawn according to the oxidation weight gained and oxidation time per unit area by discontinuous weight gain method, and the phase qualitative analysis of the oxidation products was carried out by X'Pert Pro multi-functional X-ray diffractometer (XRD),with Cu Kα radiation (λ = 1.5406 Å) and 2 θ scan between 20° to 90°. FEI Quanta F-type field emission scanning electron microscopy (SEM) and energy dispersive spectrometer (EDS) were used to observe the oxidized surface and cross-sectional morphology of the material.

3. RESULTS AND DISCUSSION

3.1. Oxidation kinetic analysis

Fig. 3 shows the high temperature oxidation kinetics curves of the new martensitic heat-resistant steel at 650 °C and 700 °C. As can be seen from the figure that the high-temperature oxidation kinetics curves of the new martensitic heat-resistant steel at two different temperatures are obviously divided into two stages. The first stage is the rapid oxidation stage, and the oxidation weight gain shows an upward trend; the second stage is called stable oxidation stage, where the oxidation rate significantly decreases and the oxidation weight gain trend slows down. The average oxidation rate of the steel is 0.0239 $g\cdot(m^2\cdot h)^{-1}$ after oxidation at 650 °C for 200 h and the average oxidation rate of the sample after oxidation in air at 700 °C for 200 h is 0.0418 $g\cdot(m^2\cdot h)^{-1}$.Compared with the evaluation standard of oxidation resistance level of superalloy [26], the oxidation resistance classification of the new martensitic heat-resistant steel belongs to the complete oxidation resistance category.

The oxidation kinetics curve is divided into two stages due to the different oxidation mechanism in the high temperature oxidation process. The sample is oxidized in atmospheric environment where there is sufficient oxygen. The transmission number of electrons or electron holes in the oxide film is much greater than that of ions. Therefore, the transmission speed and number of metal cations and oxygen negative ions through the oxide film become the main control factors of the oxidation process [27]. In the early stage of oxidation, the surface of the steel is smooth and exposed to the air, which is in the stage of rapid oxidation. The place where oxide nucleation is caused by defects such as grain boundary on alloy surface [28].

Table 1. Chemical composition of new martensitic heat-resistant steel (mass fraction %)

Element	Al	Cr	Mn	Ni	Mo	Cu	Si	V	Nb	C	P	S	Fe
Content	0.543	9.07	1.427	1.523	0.913	2.602	0.570	0.274	0.098	0.086	0.019	0.012	Bal.

Combined with the Fig. 7 a, b and Fig. 8 a, b below, it is observed that the density of oxide layer of new martensitic heat-resistant steel at 650 °C is lower than that at 700 °C when the oxidation time is 30 h and 80 h, which leads to more air entering into the oxide layer through small gaps, which promotes further oxidation of the sample and further acceleration of oxidation weight gain rate. In the stable oxidation stage, a layer of oxide film is formed on the surface of the test steel. The continuous growth of the oxide film depends on the diffusion and mass transfer of metal and oxygen atoms through the oxide layer. The oxidation process is controlled by the element diffusion mechanism, and the oxidation rate is significantly reduced [29]. During the oxidation process at 650 °C, the oxidation rate of the new martensitic heat-resistant steel is slow and a dense continuous oxide film cannot be formed rapidly. The weight gain rate per unit area is larger within 20 hours, and then tends to increase slowly, and the weight gain rate is significantly lower than that of 20 hours before oxidation. During the oxidation process at 700 °C, the oxidation rate accelerated in the first 20 hours, forming a protective oxide film, and then the weight gain rate per unit area tended to be stable. The main reason was that the increase of temperature accelerated the migration speed of positive and negative ions through the oxide film at the initial stage of oxidation.

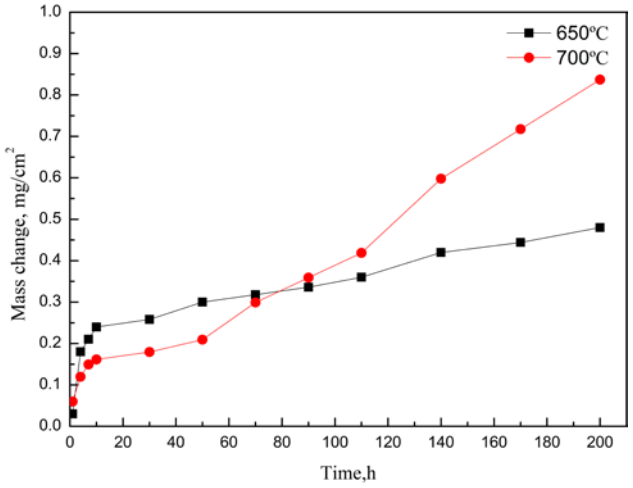

Fig. 3. High temperature oxidation kinetics curve of new martensitic heat resistant-steel

3.2. Phase analysis of oxide film

The XRD phase analysis was performed on the surface oxide film of the new martensitic heat-resistant steel after oxidation at 650 °C and 700 °C for 200 h, and the results are shown in Fig. 4. It can be seen from the figure that the main oxide on the surface of the test steel is Fe_2O_3. It also be seen that $CuFe_2O_4$ oxide exists at 700 °C, combined with the EDS in Fig. 8 d, it can be shown that the addition of Cu element to the martensitic heat-resistant steel is helpful to form $CuFe_2O_4$ oxide protective layer. According to the different intensity of diffraction peaks in XRD patterns, it was found that the oxidation of the materials was accelerated with the increase of experimental temperature.

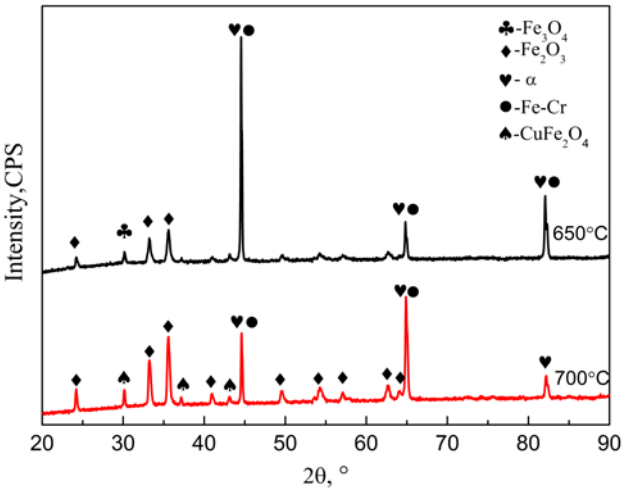

Fig. 4. XRD analysis of oxide film of new martensitic heat-resistant steel

3.3. Analysis of surface morphology of oxide film

The surface morphology characteristics of the new martensitic heat-resistant steel after oxidation at 650 °C in air for different times are shown in Fig. 5 a – d and the results of EDS composition analysis in micro region are shown in Table 2. As can be seen from the figure that during the high temperature oxidation at 650 °C, the surface morphology changes from complex rhombic shape, needle shape and granular shape to spherical shape, and then from spherical shape to more uniform irregular block shape. After oxidation for 200 h, the oxide film of new martensitic heat-resistant steel presents irregular block distribution, with large grain size and uniform distribution. The surface oxide film of new martensitic heat-resistant steel was analyzed by EDS at 650 °C in air. The oxidation of 30 h is in the primary stage of oxidation. The protective oxide of Al, Si and Cr elements is formed in the surface film, but less content is not enough to form a continuous and compact oxide film. EDS analysis of the oxide film after 80 h and 140 h oxidation showed that the content of Mo in the oxide film was as high as 20 %, MoO_3 appears on the oxide surface in a globular state as show in Fig. 5 c. Different from the morphology after high temperature oxidation for 30 h and 200 h, only 2.42 % of the oxide film was oxidized for 30 h, while no Mo element was found in the oxide film after 200 h oxidation. Mo element will form a dense adhesive oxide film above 475 °C, and the oxidation rate depends on the diffusion speed of metal ions and oxygen through the oxide film. Generally, the oxidation rate is slow at this stage. When the oxide film is formed a 600 °C, MoO_3 will evaporate. With the increase of temperature, the evaporation speed will be accelerated, and no oxide film will be formed above 700 °C, but it will volatilize directly [30].

Table 2. EDS table of new martensitic heat-resistant steel oxidized at 650 °C for different time

Time, h	Element	O	Al	Si	Nb	Mo	V	Cr	Mn	Fe	Ni	Cu
30	wt.%	22.32	0.92	1.08	0.61	2.42	0.68	24.37	6.74	31.82	1.09	7.96
80	wt.%	19.30	0.94	0.46	2.28	22.63	0.60	12.09	9.15	25.66	1.00	5.88
140	wt.%	22.51	0.27	0.23	1.82	20.88	0.87	3.96	5.50	34.58	0.89	8.50
200	wt.%	22.15	0.73	0.44	0.51	0.00	0.52	22.90	6.74	34.59	0.46	10.95

Table 3. EDS table of new martensitic heat-resistant steel oxidized at 700 °C for different time

Time, h	Element	O	Al	Si	Nb	Mo	V	Cr	Mn	Fe	Ni	Cu
30	wt.%	22.06	0.86	0.73	0.12	0.34	0.68	16.91	6.06	42.28	0.69	9.26
80	wt.%	21.58	0.43	0.56	0.40	0.32	0.93	17.79	6.00	40.46	1.45	10.08
140	wt.%	21.19	0.66	0.50	0.00	0.00	0.55	14.84	5.52	42.94	1.11	12.71
200	wt.%	24.04	3.16	0.84	0.41	0.36	0.45	32.30	9.85	12.84	0.20	15.56

Therefor, the surface morphology is spherical when the oxidation time is 80 h and 140 h. When the oxidation time reaches 200 h, MoO_3 volatilizes directly and the surface morphology is irregular and massive.

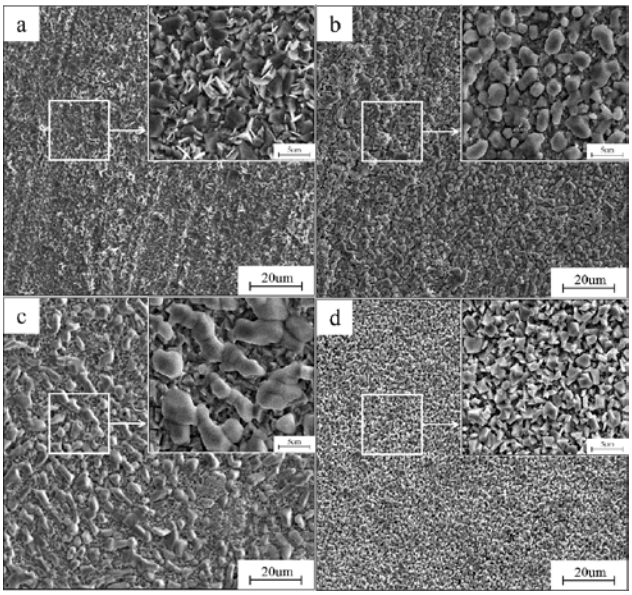

Fig. 5. Surface morphology characteristics of new martensitic heat-resistant steel after high temperature oxidation in air at 650 °C for different time: a – 30 h; b – 80 h; c – 140 h, d – 200 h

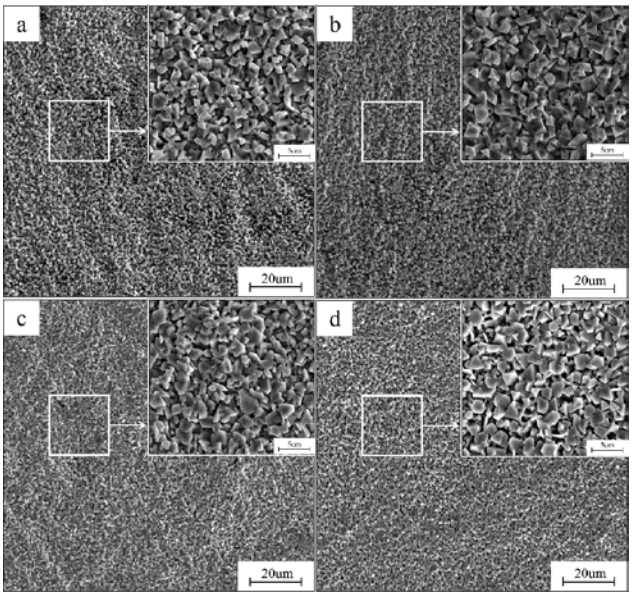

Fig. 6. Surface morphology characteristics of new martensitic heat-resistant steel after high temperature oxidation in air at 700 °C for different time: a – 30 h; b – 80 h; c – 140 h; d – 200 h

The surface morphology characteristics of the new martensitic heat-resistant steel after oxidation at 700 °C in air for different times are shown in Fig. 6 a – d and the results of EDS composition analysis in micro region are shown in Table 3.

Under 700 °C air environment, the surface oxidation morphology of the new martensitic heat-resistant steel presents uneven size and irregular distribution of blocky. With the increase of oxidation time, the oxide grains of the surface oxide film gradually grow, and the shape remains massive, and the distribution is more dense. Selective oxidation exists in the oxidation process at 700 °C and protective oxides formed by Al, Si and Cr elements still exist on the surface oxide film after oxidation at 700 °C for 30 h. The oxidation rate between 30 h and 80 h is higher than that at 650 °C, and the time of stable oxidation is earlier than that at 650 °C. From the EDS results, it can be seen that the content of Cu element on the surface of the oxide film increases gradually. CuO or CuO_2 is formed by copper oxidation, which makes the volume increase. The compressive stress causes local damage of the oxide layer, and the non oxidized area is exposed to the air again to oxidize [31], which also leads to the oxide size larger than that oxidized at 650 °C for 200 h.

3.4. Analysis of oxidation cross-section

Fig. 7 shows the cross-section morphology and EDS line scanning element distribution of the oxide film of the new martensitic heat-resistant steel after oxidation in air at 650 °C for different time. The average thickness of oxidation film of new martensitic heat-resistant steel is 22 um, 25 um, 29 um and 49 um after 30 h, 80 h, 140 h and 200 h respectively. With the increase of oxidation time, the thickness of oxide film increases gradually. The increasing trend of thickness is obvious at 30 h, and slows down from 30 h to 140 h. The increasing trend is obvious from 140 h to 200 h, which is consistent with the oxidation kinetics curve at 650 °C. It can be seen from the figure that with the increase of oxidation time, a large number of holes and cracks appear in the oxide film, and the density also decreases. After oxidation for 200 h, the structure of the oxide film is obviously divided into two layers, the outer layer is loose and porous, and the protection is weak, while the inner layer is dense and tightly combined with the matrix, which plays a good protective role. The outer oxide film is mainly composed of Fe and Cu oxides, while the inner oxide film contains Al_2O_3, SiO_2 and Cr_2O_3 protective oxides formed by Al, Si and Cr elements. The diffusion rate of Cr is much slower than that of Fe [32]. In the oxidation process, the element distribution in the inner oxidation layer and the inner oxide layer can be seen. The content of Cr in the oxidation layer is obviously higher than that in the middle layer. It cannot form a continuous nodal Cr rich area in time, which hinders the internal diffusion of O or the outward diffusion channel and speed of Fe, and slows down the growth of new oxides [33, 34].

A large amount of Fe element is missing in the inner oxide film, which is mainly caused by the continuous outward diffusion of iron ions in the high temperature oxidation process to form FeO unprotected oxide film [35]. Cr is oxidized to form continuous and complete Cr_2O_3 protective oxide film [36]. The Cr_2O_3 in the inner oxide film effectively prevents further oxidation of the metal matrix. At the same time, SiO_2 has excellent microstructure stability at high temperature, which can increase the compactness of Cr_2O_3 oxide film and inhibit the exfoliation of Cr_2O_3 oxide film [37].

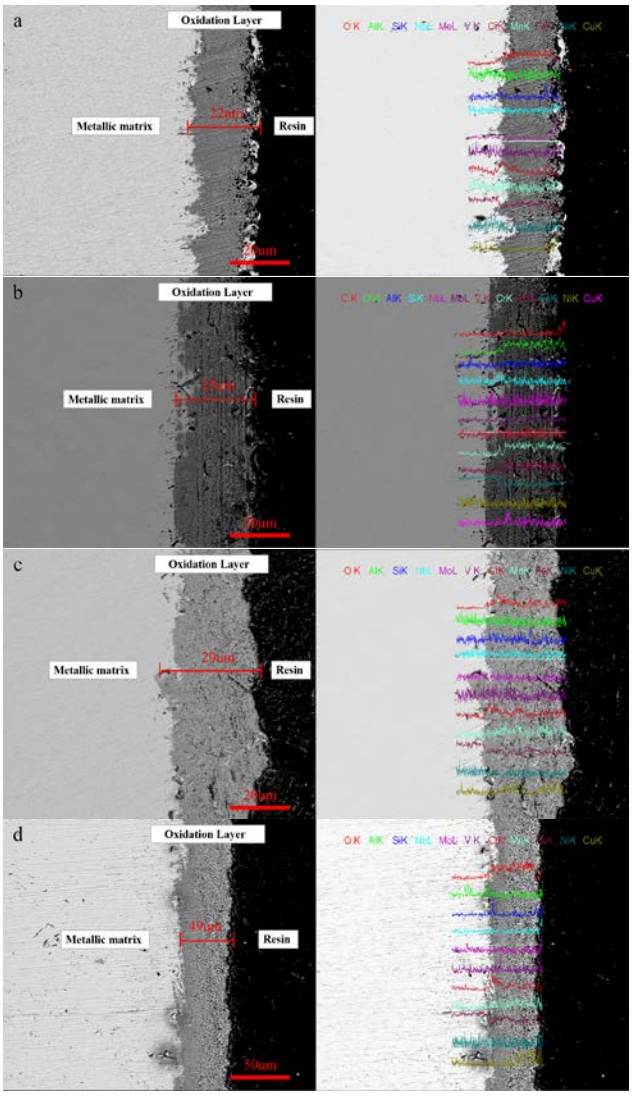

Fig. 7. Cross-section morphology and EDS analysis of new martensitic heat-resistant steel after high temperature oxidation in air at 650 °C for different time: a – 30 h; b – 80 h; c – 140 h; d – 200 h

Fig. 8 shows the cross-sectional morphology and element distribution of the oxide film of the new martensitic heat-resistant steel after oxidation at 700 °C in air for different time. The results show that the thickness of oxidation film increases with the increase of oxidation time, which is consistent with the weight increasing trend of oxidation kinetics curve. Compared with the morphology of oxide film oxidized at 650 °C, the thickness of oxide film increases and the density is better. At 700 °C, the selective oxidation is obvious at the initial stage of oxidation. After 30 h oxidation at 700 °C in air, the oxide film is very dense, and the protective oxide film is composed of Cr_2O_3 protective oxide. As the oxidation process continues, the protective oxide film was damaged, and voids and cracks began to appear.

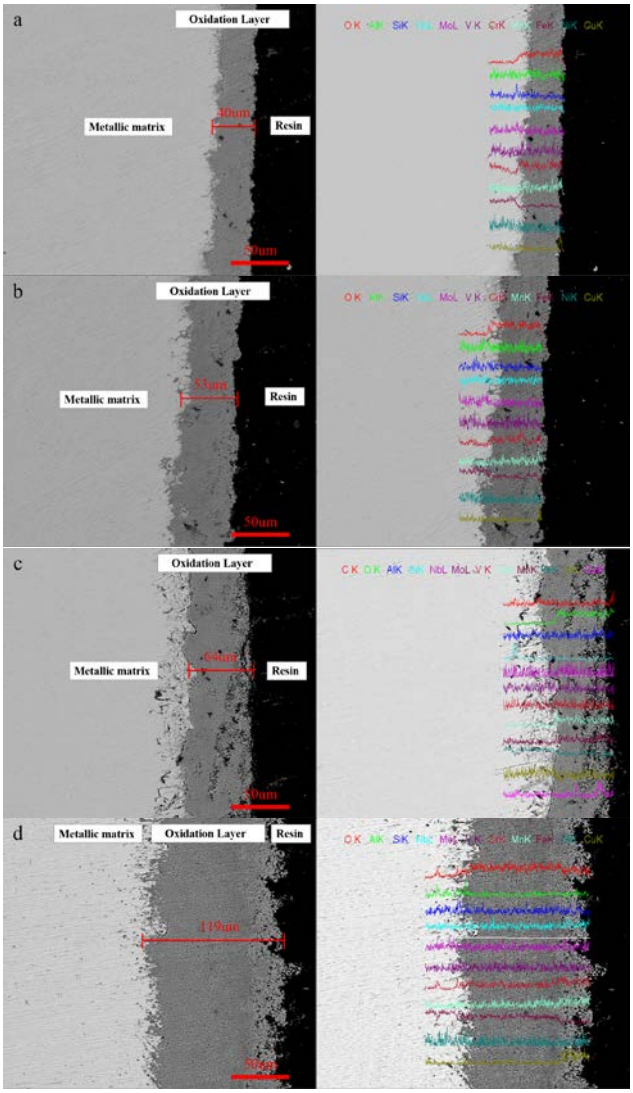

Fig. 8. Cross-section morphology and EDS analysis of new martensitic heat resistant-steel after high temperature oxidation in air at 700 °C for different time: a – 30 h; b – 80 h; c – 140 h; d – 200 h

Combined with Fig. 6 b, it can be seen that there are voids and pits in the oxide layer, With the increase of oxidation time, the oxide film transformed into a double-layer oxide film with loose and porous outer layer and dense inner layer with strong protection. According to the element distribution of the oxide film cross section of the test steel, after oxidation at 700 °C for 200 h, the outer layer of the oxide film is mainly composed of Cu, Fe and Mn elements, while the inner layer is mainly composed of Cr, Al and Si oxides. The Cr_2O_3 oxide film is usually continuous and dense, which has protective effect on the material. However, when Cr_2O_3 exists with CuO, they will interlace with each other and form discontinuous structure easily, leading to the damage of the original protective Cr_2O_3 oxide film and then promoting further oxidation. After oxidation at 700 °C for 200 h, the outer oxide film of

the test steel is sparse and porous, which is caused by the interlacing of Cr_2O_3 and CuO [38]. The outer oxide film is loose and porous, which leads to oxygen entering into the inner layer and further oxidizes the internal oxide layer. The element of Cr is mainly concentrated near the inner layer, which makes the inner oxide layer compact and achieves good antioxidant effect.

4. CONCLUSIONS

The new martensitic heat-resistant steel with a small amount of Al and Cu elements shows excellent high-temperature oxidation resistance after oxidation at 650 °C and 700 °C for 200 h in air environment, and its oxidation resistance level belongs to complete oxidation resistance level. In the process of high temperature oxidation, the oxide film of the new martensitic heat-resistant steel changes from one-layer structure to two-layer structure with loose outer layer and dense inner layer. In the process of oxidation, aluminum, silicon, chromium and manganese are preferentially oxidized compared with iron, forming a protective oxide film to reduce the oxidation of iron and protect the matrix.

Acknowledgments

This research was Supported by Key Laboratory fund general projects (No. 6142905180203).

REFERENCES

1. **Hong, L., Zhao, C.Z., Tao, Y., Zhang, H.X.** Properties of High Temperature Oxidation of Heat-resistant Steel with Aluminum and Copper *Materials Science (Medžiagotyra)* 25 (4) 2019: pp. 394 – 400. https://doi.org/10.5755/j01.ms.25.4.195
2. **Tang, F., Dong, B., Zhao, M.** USC Unit Development and Application in China *Electric Power Construction.* 31 (1) 2010: pp. 80 – 82.
3. **Xu, T.M., Yuan, Y.C., Chen, G.J.** Developmental Trend of Super-large Capacity and Ultra Supercritical Boilers *Power Engineering.* 23 2003: pp. 63 – 65.
4. **Liu, J.R.** The Analysis and Optimization Program about Energy-saving Potential of Ultra-supercritical Boiler Unit. Beijing: North China Electric Power University, PhD thesis , 2010.
5. **Kritzer, P.** Corrosion in High-Temperature and Supercritical Water Andaqueous Solutions: A Review *Journal of Supercritical. Fluids* 29 2004: pp. 1 – 29. https://doi.org/10.1016/S0896-8446(03)00031-7
6. **Zhang, D.Q., Xu, J.J., Zhao, G.Q.** Oxidation Characteristic of Ferritic-Martensitic Steel T91 Ii Water-vapour Atmosphere *Chinese Journal of Materials Research.* 22 2008: pp. 599 – 605.
7. **Li, Z.G.** Study on High Temperature Oxidation of Water Vapor. Xi'an: Xi'an Thermal Power Research Institute Co. Ltd., 2006.
8. **Liu, J., Ding, S.F.** Evaluation Research on Iron Scale Generation Ofhigh Temperature Heat Surfaces in Supercritical Boiler. Shanghai:Shanghai Power Equipment Research Institute, PhD thesis, 2013.
9. **Xia, T.F., Zhang, D.Q., Gao, L.X.** Advances in High Temperature Steam Oxidation Behavior and Control Technology of Heat Resistant Steel *Corrosion Sciencea and Protcetion Technology.* 27 2015: pp. 199 – 202.
10. **Li, J.R., Liu, S.Z., Wang, X.G.** Development of a Low Cost Third Generation Single Crystal Superalloy DD9 Superalloys. John Wiley & Sons, Ltd. 2016. https://doi.org/10.1002/9781119075646.ch6
11. **Chi, Ch., Yu, H., Dong, J.** Strengthening Effect of Cu-rich Phase Precipitation in 18Cr9Ni3CuNbN Austenitic Heat-resisting Steel *Acta Metallurgica Sinica* 24 (2) 2011: pp. 141 – 147. https://doi.org/10.11890/1006-7191-112-141
12. **Arivazhagan, B., Vasudevan, M.** A Study of Microstructure and Mechanical Properties of Grade 91 Steel A-TIG Weld Joint *Journal of Materials Engineering and Performance* 22 (12) 2013: pp. 3708 – 3716. https://doi.org/10.1007/s11665-013-0694-9
13. **Brady, M.P., Wright, I.G., Gleeson, B.** Alloy Design Strategies for Promoting Protective Oxide-scale Formation *Journal of Metals* 52 (1) 2000: pp. 16 – 21. https://doi.org/10.1007/s11837-000-0109-x
14. **Airiskallio, E., Nurmi, E., Heinonen, M.H.** High Temperature Oxidation of Fe–Al and Fe–Cr–Al alloys: The Role of Cr as a Chemically Active Element *Corrosion Science* 52 (10) 2010: pp. 3394 – 3404. https://doi.org/10.1016/j.corsci.2010.06.019
15. **Osgerby, S., Fry, A.T.** The Role of Alloy Composition on the Steam Oxidation Resistance of 9-12%Cr Steels *Materials Science Forum* 2006: pp. 129 –138. https://doi.org/10.4028/www.scientific.net/MSF.522-523.129
16. **Yamamoto, Y.** Alumina-Forming Austenitic Stainless Steels Strengthened by Laves Phase and MC Carbide Precipitates *Metallurgical and Materials Transactions A* 38 (11) 2007: pp. 2737 – 2746. https://doi.org/10.1007/s11661-007-9319-y
17. **Spindler, S., Wittmann, R., Gerthsen, D.** Dislocation Properties of Polycrystalline Fe–Cr–Al Alloys and their Correlation with Mechanical Properties *Materials Science & Engineering A (Structural Materials:, Properties, Microstructure and Processing)* 289 (1 – 2) 2000: pp. 151 – 161. https://doi.org/10.1016/S0921-5093(00)00910-2
18. **Song, J.L., Lin, S.B., Yang, C.L.** Spreading Behavior and Microstructure Characteristics of Dissimilar Metals TIG Welding-brazing of Aluminum Alloy to Stainless Steel *Materials Science and Engineering A* 509 (1) 2009: pp. 31 – 40. https://doi.org/10.1016/j.msea.2009.02.036
19. **Takahashi, A., Iino, M.** Microstructural Refinement by Cu Addition and its Effect on Strengthening and Toughening of Sour Service Line Pipe Steels *ISIJ International* 36 (2) 1996: pp. 241 – 245.
20. **Zhu, L., Hu, M., Ni, W.** High Temperature Oxidation Behavior of Ti0.5Al0.5N Coating and Ti0.5Al0.4Si0.1N coating *Vacuum* 86 (12) 2012. https://doi.org/10.1016/j.vacuum.2012.04.013
21. **Jianian, S., Longjiang, Z., Tiefan, L.** High-temperature Oxidation of Fe-Cr Alloys in Wet Oxygen *Oxidation of Metals* 48 (3/4) 1997: pp. 347 – 356. https://doi.org/10.1007/BF01670507
22. **Kan, T., Sawaragi, Y., Yamadera, Y., Okada, H.** Properties and Experiences of a New Austenitic Stainless Steel Super304H(0.1C-18Cr–9Ni–3Cu–Nb–N) for Boiler Tube Application *Materials for Advanced Power Engineering* 1998: pp. 441 – 450.

23. **Park, D., Huh Moo, Y., Jung Woo, S., Suh, J.Y., Shim Jae, H., Lee, S.** Effect of Vanadium Addition on the Creep Resistance of 18Cr9Ni3CuNbN Austenitic Stainless Heat Resistant Steel *Journal of Alloys and Compounds.* 574 2013: pp. 532 – 538. https://doi.org/10.1016/j.jallcom.2013.05.106
24. **Iseda, A., Okada, H., Semba, H., Igarashi, M.** Long Term Creep Properties and Microstructure of Super304H, TP347HFG and HR3C for A-USC Boilers *Energy Mater* 2 2007: pp. 199 – 206.
25. **Zhang, Y., Zhu, L., Qi, A., Lu, Z.** Microstructural Evolution and the Effect on Mechanical Properties of S30432 Heat-resistant Steel During Aging at 650 °C *ISIJ International.* 50 2010: pp. 596 – 600. https://doi.org/10.2355/isijinternational.50.596
26. Test Method for Determination of Oxidation Resistance of Steels and Super Alloys, Industry Standard – Aviation. HB 5258-2000, Test Method for Determination of Oxidation Resistance of Steel and High-Temperature Alloys, Standard.
27. **Brückman, A.** The Mechanism of Transport of Matter Through The Scales During Oxidation of Metals And Alloys *Corrosion Science* 7 (1) 1967: pp. 51 – 59. https://doi.org/10.1016/S0010-938X(67)80069-6
28. **Wang, H., Zhao, Q., Yu, H.** Effect of Aluminium and Silicon on High Temperature Oxidation Resistance of Fe-Cr-Ni Heat Resistant Steel *Transactions of Tianjin University* 15 (6) 2009: pp. 457 – 462. https://doi.org/10.1007/s12209-009-0079-1
29. **Huntz, A.M., Reckmann, A., Haut, C.** Oxidation of AISI 304 and AISI 439 Stainless Steels *Materials Science & Engineering A* 447(1 – 2) 2007: pp. 266 – 276. https://doi.org/10.1016/j.msea.2006.10.022
30. **Natesan, K, Deevi, S.C.** Oxidation Behavior of Molybdenum Silicides and their Composites *Intermetallics* 8 (9 – 11) 2000: pp. 1147 – 1158. https://doi.org/10.1016/s0966-9795(00)00060-1
31. **Gesmundo, F., Niu, Y.** The Internal Oxidation of Ternary Alloys I: The Single Oxidation of the Most-Reactive Component Under Low Oxidant Pressures *Oxidation of Metals* 60 (5 – 6) 2003: pp. 347 – 370. https://doi.org/10.1023/A:1027398104508
32. **Martinelli, L., Balbaud-Celerier, F., Terlain, A.** Oxidation Mechanism of a Fe–9Cr–1Mo Steel by Liquid Pb–Bi Eutectic Alloy (Part I) *Corrosion Science* 50 (9) 2008: pp. 2523 – 2536. https://doi.org/10.1016/j.corsci.2008.06.050
33. **Robertson, J.** The Mechanism of High Temperature Aqueous Corrosion of Stainless Steels *Corrosion Science* 32 (4) 1991: pp. 443 – 465. https://doi.org/10.1016/0010-938X(91)90125-9
34. **Yan, G, Jian-Min, J., Shu-Fang, H, Tang Li-ying** Steam Oxidation Behavior of Domestic TP347H FG Steel *Corrosion Science & Protection Technology* 23 (6) 2011: pp. 506 – 509.
35. **Liu, G., Wang, C., Yu, F, Tian, J.** Evolution of Oxide Film of T91 Steel in Water Vapor Atmosphere at 750°C *Oxidation of Metals* 81 (3 – 4) 2014: pp. 383 – 392. https://doi.org/10.1007/s11085-013-9448-1
36. **Ul-Hamid, A, Mohammed, A.I., Al-Jaroudi, S.S., Tawancy, H.M., Abbas, N.M.** Evolution of Oxide Scale on A Ni-Mo-Cr Alloy at 900 °C *Materials Characterization* 8 (1) 2007: pp. 13 – 23. https://doi.org/10.1016/j.matchar.2006.03.005
37. **Am, H., Bague, V., Beauple, G., Haut, C., Severac, C., Lecour, P., Longaygue, X., Ropital, F.** Effect of Silicon on the Oxidation Resistance of 9% Cr Steels *Applied Surface Science* 207 (1 – 4) 2003: pp. 255 – 275. https://doi.org/10.1016/S0169-4332(02)01505-2
38. **Bamba, G., Wouters, Y., Galerie, A., Charlot, F., Dellali, A.** Thermal Oxidation Kinetics and Oxide Scale Adhesion of 15Cr Alloys in Function of their Silicon Content *Acta Materialia* 54 (15) 2006: pp. 3917 – 3922. https://doi.org/10.1016/j.actamat.2006.04.023